Targeting the effector domain of the myristoylated alanine rich C-kinase substrate enhances lung cancer radiation sensitivity

TIMOTHY D. ROHRBACH[1], JOHN S. JARBOE[1], JOSHUA C. ANDERSON[1], HOA Q. TRUMMELL[1], PATRICIA H. HICKS[1], ALICE N. WEAVER[1], EDDY S. YANG[1], ROBERT A. OSTER[2], JESSY S. DESHANE[3], CHAD STEELE[3], GENE P. SIEGAL[4], JAMES A. BONNER[1] and CHRISTOPHER D. WILLEY[1]

[1]Department of Radiation Oncology; [2]Division of Preventive Medicine and [3]Division of Pulmonary, Allergy and Critical Care Medicine, Department of Medicine; [4]Department of Pathology, The University of Alabama at Birmingham, Birmingham, AL, USA

Received September 30, 2014; Accepted November 7, 2014

DOI: 10.3892/ijo.2014.2799

Abstract. Lung cancer is the leading cause of cancer related deaths. Common molecular drivers of lung cancer are mutations in receptor tyrosine kinases (RTKs) leading to activation of the phosphatidylinositol 3-kinase (PI3K)/Akt pro-growth, pro-survival signaling pathways. Myristoylated alanine rich C-kinase substrate (MARCKS) is a protein that has the ability to mitigate this signaling cascade by sequestering the target of PI3K, phosphatidylinositol (4,5)-bisphosphate (PIP_2). As such, MARCKS has been implicated as a tumor suppressor, though there is some evidence that MARCKS may be tumor promoting in certain cancer types. Since the MARCKS function depends on its phosphorylation status, which impacts its subcellular location, MARCKS role in cancer may depend highly on the signaling context. Currently, the importance of MARCKS in lung cancer biology is limited. Thus, we investigated MARCKS in both clinical specimens and cell culture models. Immunohistochemistry scoring of MARCKS protein expression in a diverse lung tumor tissue array revealed that the majority of squamous cell carcinomas stained positive for MARCKS while other histologies, such as adenocarcinomas, had lower levels. To study the importance of MARCKS in lung cancer biology, we used inducible overexpression of wild-type (WT) and non-phosphorylatable (NP)-MARCKS in A549 lung cancer cells that had a low level of endogenous MARCKS. We found that NP-MARCKS expression, but not WT-MARCKS, enhanced the radiosensitivity of A549 cells in part by inhibiting DNA repair as evidenced by prolonged radiation-induced DNA double strand breaks. We confirmed the importance of MARCKS phosphorylation status by treating several lung cancer cell lines with a peptide mimetic of the phosphorylation domain, the effector domain (ED), which effectively attenuated cell growth as measured by cell index. Thus, the MARCKS ED appears to be an important target for lung cancer therapeutic development.

Correspondence to: Dr Christopher D. Willey, Department of Radiation Oncology, The University of Alabama at Birmingham, 619 19th St. South, HSROC 2232C, Birmingham, AL 35249, USA
E-mail: cwilley@uab.edu

Key words: MARCKS, lung cancer, phosphorylation, radiation therapy

Introduction

Myristoylated alanine rich C-kinase substrate (MARCKS) has been described as having contradicting roles in cancer biology. Studies of MARCKS in colon cancer, melanoma, prostate cancer, hepatocellular carcinoma as well as glioblastoma multiforme (GBM) have indicated that MARCKS behaves as a tumor suppressor (1-5). In contrast, studies in breast cancer and choloangiocarcinoma have suggested that MARCKS expression correlates with poor prognosis (6,7). Collectively, this information highlights the importance of the cellular environment in driving MARCKS signaling. The significance of MARCKS signaling with respect to growth and response to treatment of lung cancer is under investigation.

Common drivers of lung cancer include the fusion protein, anaplastic lymphoma kinase (ALK), and mutations and hyperactivation of receptor tyrosine kinases (RTKs) such as: epidermal growth factor receptor (EGFR), c-MET (hepatocyte growth factor receptor, HGFR), insulin growth factor receptor 1 (IGF-1R) and fibroblast growth factor receptor (FGFR) (8). RTKs phosphorylate and activate phosphatidylinositol 3-kinase (PI3K) which then phosphorylates phosphatidylinositol (4,5)-bisphosphate (PIP_2) producing phosphatidylinositol (3,4,5)-triphosphate (PIP_3) (9). PIP_3 serves as an anchoring and activation site for the pleckstrin homology (PH) domain of the pro-growth, pro-survival kinase, Akt, among others (10). Importantly, MARCKS contains an effector domain (ED) capable of binding to the plasma membrane through an electrostatic interaction with PIP_2 molecules, thereby sequestering them (11,12) and preventing their conversion to PIP_3. This can effectively attenuate Akt activity. However, when the MARCKS ED is bound by calcium-calmodulin or phosphorylated by serine kinases such as protein kinase C (PKC) or Rho-associated coiled-coil kinase (ROCK), MARCKS releases PIP_2 at the plasma membrane and migrates into the

cytoplasm due to electrostatic repulsion by the phosphate groups (13,14), though this is reversible through phosphatase action (15).

MARCKS is expressed in human lung tissue; however, investigation of MARCKS involvement in lung cancer biology is limited (16). Hanada *et al* (17) found that MARCKS expression may provide a possible biomarker and prognostic indicator for human squamous cell carcinoma of the lung. MARCKS expression was increased in tumor tissue compared to adjacent normal tissue, and high MARCKS expression by immunohistochemistry (IHC) was associated with poor prognosis. Additionally, Chen *et al* (18) described MARCKS being expressed in higher levels in non-small cell lung cancer (NSCLC) compared to normal tissue. Using a peptide mimetic targeting the N-terminal region of MARCKS, they were able to reduce migration in *in vitro* as well as *in vivo* models.

In the present study, we investigated MARCKS expression in multiple lung tumor pathologies. Moreover, we examined the importance of MARCKS and selected MARCKS mutants in terms of lung cancer cell phenotype, particularly in response to ionizing radiation. Our data suggest a critical dependence of the phosphorylation status of the MARCKS effector domain (ED) with respect to radiosensitization.

Materials and methods

Cell culture. Human lung cancer cell lines A549, H1299, H1792 and H1975 (American Type Culture Collection, Manassas, VA, USA) were cultured in RPMI-1640 with 10% fetal bovine serum (FBS), 1% penicillin-streptomycin (pen-strep) and 1% GlutaMAX (Invitrogen/Life Technologies, Grand Island, NY, USA). 293FT human embryonic kidney cells (Invitrogen/Life Technologies) were cultured in Dulbecco's modified Eagle's medium (DMEM) with 10% FBS and 1% pen-strep. All cells were maintained at 37˚C in 5% CO_2.

Immunohistochemical tissue array. A lung tumor tissue microarray (TMA) (cat. #BC041114) was purchased from US Biomax, Inc. (Rockville, MD, USA). The TMA was deparaffinized in xylene followed by 100, 95 and 70% graded ethanol solutions and rehydrated in dH_2O. Endogenous peroxidase was blocked by a 5-min incubation with 3% hydrogen peroxide solution in phosphate-buffered saline (PBS). The TMA was then incubated with sodium citrate buffer (Dako, Carpinteria, CA, USA) for 20 min for antigen retrieval. Non-specific interactions were blocked in 20-min incubation (room temperature) in 5% bovine serum albumin (BSA), 100 mM Tris (pH 8.2 to 8.5) solution. MARCKS was stained with an anti-MARCKS primary antibody (EP1446Y, 1 h at room temperature; Abcam, Cambridge, MA, USA) followed by an anti-rabbit alkaline phosphatase (AP) conjugated secondary antibody (Invitrogen; 1 h at room temperature). Following the manufacturer's protocols, Vector Red (Vector Laboratories, Inc., Burlingame, CA, USA) was used to detect MARCKS. Cells were counterstained with 1% methyl green solution. Lastly, the TMA was dehydrated using 70% ethanol, 50/50 ethanol/xylene, 100% xylene gradations and coverslip mounted using PROTOCOL SecureMount (cat. #23-022-208; Thermo Fisher Scientific, Waltham, MA, USA). Images were captured using a Zeiss Observer A1 microscope using an AxioCam MRc 5 camera. A board certified pathologist scored each tissue in a blinded fashion using a scale of 0, 0.5, 1, 2 or 3 with 0 equaling no detection and 3 being the highest intensity. The highest ethical standards were followed while collecting and handling patient tumors and information. Informed consent was obtained from each patient before tumor collection.

Generation of lentiviral MARCKS constructs and packaging plasmids. The ViraPower HiPerform T-REx Gateway Expression System (cat. #A11141) and the pENTR221 entry vector (pENTR221-MARCKS) containing the wild-type (WT) MARCKS sequence were purchased from Invitrogen. The WT-MARCKS sequence from pENTR221-MARCKS was cloned into the pLenti6.3/TO/V5-DEST destination vector using Clonase from the Gateway expression system per the manufacturer's protocol to yield pLenti6.3/TO/V5-MARCKS-WT. The non-phosphorylatable (NP) MARCKS construct, in which the 4 serines of the ED were changed to alanines, was synthesized by GenScript (GenScript USA, Inc., Piscataway, NJ, USA) and cloned into the pUC57 vector. The psPAX2 packaging plasmid (Addgene plasmid 12260; Addgene, Cambridge MA, USA) and pCMV-VSV-G envelope plasmid (Addgene plasmid 8454) were obtained from Addgene.

Viral vector production. 293FT cells ($1.5x10^6$) were plated in 7 ml of DMEM supplemented with 10% FBS without antibiotics onto a poly-D-lysine (cat. #P7886; Sigma) coated 10-cm dish. Lipofectamine 2000 (27 μl) (cat. #11668; Invitrogen) was combined with 1.5 ml Opti-MEM media (cat. #11058; Invitrogen) and incubated for 5 min at room temperature. An additional aliquot of 1.5 ml Opti-MEM media had 4 μg of psPAX2, PCMV-VSV-G, and appropriate lentiviral vector plasmid added. The plasmid and Lipofectamine media were mixed together and incubated for 20 min at room temperature. The Lipofectamine-plasmid mixture was added to the 293FT cells and incubated overnight. The following morning, media was replaced with fresh DMEM supplemented with 10% FBS and 1% pen-strep. Lentiviral supernatant was collected at 24 h, filtered through a 0.45-μm filter, aliquoted and stored at -80˚C. The QuickTiter p24 ELISA (Cell Biolabs, Inc., San Diego, CA, USA) was used to quantify lentivirus aliquots (3).

Stable cell line selection. A549 cells ($5x10^5$) were plated in 6-well plates and allowed to adhere overnight. The following morning, similar amounts of p24 quantified lentiviral particles containing tetracycline-repressor (TetR) plasmid was used to infect the cells. The cells were incubated with 500 μl of virus for 2 h, at 37˚C, in 5% CO_2 followed by 3-day incubation in growth media. Following 3 passages with 200 μg/ml geneticin (G418; Life Technologies), A549 TetR cells were re-plated on 6-well plates at $5x10^5$ cells/well for MARCKS lentiviral infection. An identical procedure as described above was performed for MARCKS virus infection, except selection was with 8 μg/ml blasticidin (Life Technologies). The tetracycline homologue, doxycycline (2 μg/ml) was used to induce expression.

MARCKS peptide design. MARCKS-ED TAT peptide was designed by conjugating the cell permeable HIV Tat peptide

(cat. #61214; Anaspec, Fremont, CA, USA) via disulfide linkage to the 25 amino acid ED sequence (KKKKKRFSFKKSFK LSGFSFKKNKK) (19). The control sequence was designed using the Expasy random peptide generator (http://www.expasy.org/randseq) using the average amino acid composition computed from Swiss-Prot (CEIEEHAWNTVEMFSSF PGTQLYNDA) to control for size of the peptide. To eliminate the positive charge effect, lysine and arginine residues were changed to glutamates and then conjugated with the HIV Tat peptide. The lyophilized peptides were re-suspended in sterile ddH_2O at a stock concentration of 5 mM to be used for the experiments.

iCELLigence assay. The iCELLigence platform (ACEA Biosciences, Inc., CA, USA) was used to monitor the cell response to doxycycline and radiation, by measuring real-time changes in cellular impedance (20,21). Cells were plated in duplicate and allowed to attach under identical conditions, either overnight or for 7 h, before doxycycline addition. In the case of radiation, both sham and radiation therapy (RT) plates were removed from the incubator after exposure for the same duration. For studies with MARCKS-ED peptide, lung cancer cells were plated for 6 h before the addition of MARCKS-ED peptide mimetic or control peptide.

Immunoblotting. Immunoblotting was performed as previously described (3). Briefly, cells were lysed using MPER lysis buffer supplemented with protease (cat. #P8340; Sigma-Aldrich, St. Louis, MO, USA) and phosphatase inhibitors (Sigma-Aldrich #P0044 and P5726). Samples were separated by electrophoresis through either an 8 or 10% SDS-polyacrylamide gel (SDS-PAGE) and transferred to a PVDF membrane (Immobilon; EMD Millipore, Billerica, MA, USA). Blots were blocked in 5% milk, 1% BSA and probed with the following antibodies at the manufacturer's recommended concentrations: phospho-MARCKS (Abcam ab81295), MARCKS (Abcam ab52616), phospho-Akt (S473) (cat. #D9E, #4060; Cell Signaling Technology, Danvers, MA, USA), phospho-Akt (T308) (Cell Signaling Technology C31E5E, #2965), Akt (Cell Signaling Technology C67E7, #4691), actin (Santa Cruz Biotechnology, sc-1616), and V-5 (Invitrogen, R96125).

Clonogenic assay. Cells were diluted and plated in defined numbers to give six replicates per treatment condition. After 6 h, the media was changed (with or without doxycycline) and incubated overnight. The following morning, cells were treated with 0, 3, 5 or 8 Gy of irradiation using a 320 kV X-ray irradiator (Kimtron, Inc., Woodbury, CT, USA). After one week, cells were fixed and stained with 6.0% glutaraldehyde and 0.5% crystal violet. Colonies consisting of 50 or more cells were counted for each condition. A surviving fraction (S.F.) was calculated by using the equation (number of colonies formed/number of cells plated)/(number of colonies for sham irradiated group/number of cells plated). The result was plotted as the mean and the standard error of the mean in a semi-logarithmic format (22,23). The dose enhancement ratio (DER) was calculated as the dose (Gy) for the non-induced A549 cells (doxycycline absent) divided by the dose for induced A549 cells (doxycycline supplemented) for which a survival fraction of 0.2 was achieved.

Senescence associated β-galactosidase staining. β-galactosidase was used as a marker for senescence using the Cell Signal kit (cat. #9860). Cells were plated, attached overnight, and then treated overnight with or without doxycycline. Cells were exposed to 5 Gy and stained 1 week following irradiation. The manufacturer's protocol was followed and images were captured on a Zeiss Observer A1 microscope using an AxioCam MRc 5 camera. Five representative images per condition were captured.

Mitotic catastrophe assay. Lung cancer cells were plated, attached overnight, and then treated overnight with or without doxycycline. Cells were exposed to 5 Gy of irradiation and fixed with 4% paraformaldehyde 0, 24, 48, 72 and 96 h following irradiation. Fixed cells were stained with 300 ng/ml DAPI for 10 min and washed 3 times with PBS. Nine representative images per condition were captured using a Zeiss Observer A1 microscope using an AxioCam MRc 5 camera.

Double-strand DNA damage quantification. Lung cancer cells were plated onto sterile coverslips, attached overnight, and then treated overnight with or without doxycycline. The following day cells were treated with 8 Gy of irradiation. At the indicated time-points, cells were rinsed in PBS and incubated for 5 min, at 4˚C, in ice-cold buffer (10 mM HEPES/KOH, pH 7.4, 300 mM sucrose, 100 mM NaCl, 3 mM $MgCl_2$) supplemented with 1% protease (Sigma #P8340) and 1% phosphatase inhibitors (Sigma P0044 and P5726) followed by fixation in 70% ethanol for 15 min. The cells were blocked and incubated with primary antibodies (1:500 dilution, phospho-γH2AX Ser139, Millipore, cat. #MI-07-164). The secondary antibody was the anti-rabbit Alexa Fluor 594-conjugated antibody (1:2,000 dilution; Invitrogen). DAPI was used for nuclear staining. The coverslips were subsequently mounted onto slides with mounting media (Aqua-Poly/Mount, cat. #18606; Polysciences, Inc., Warrington, PA, USA) and analyzed via an EVOS fl digital inverted fluorescence microscope (AMG; Life Technologies). Positive and negative controls were included on all experiments. A total of 500 cells were assessed. For foci quantification, cells with >10 foci were counted as positive according to the standard procedure (24-26).

Statistics. Statistical calculations and data graphing were performed using the GraphPad Prism (GraphPad Software, Inc., La Jolla, CA, USA). ANOVA was used for assessing results in the clonogenic assay, senescence associated β-galactosidase staining assay, mitotic catastrophe assay and double-strand DNA damage quantification. All statistical tests were two-sided and were performed using a significance level of 5%.

Results

Lung tumor TMA staining for MARCKS expression. Previous reports of MARCKS in lung cancer looked at the broad group of NSCLC or squamous cell carcinomas but did not perform a comprehensive analysis (17,18). We purchased a lung tumor TMA from US Biomax, Inc. containing a total of 200 lung tissue samples comprised of 62 adenocarcinoma, 12 atypical carcinoid, 4 adenosquamous carcinoma, 8 bronchoalveolar

Table I. Patient and immunohistochemical characteristics for selective lung cancer tissue staining for anti-MARCKS.

Characteristics	Data				
Average age, years	54				
Gender, n (%)					
Male	138 (69.7)				
Female	62 (31.3)				
		Intensity			
Histology	Positives per group (%)	3 n (%)	2 n (%)	1 n (%)	0.5 n (%)
Adenocarcinoma	17/62 (27.4)	0 (0)	1 (1.6)	3 (4.8)	13 (21.3)
Atypical carcinoid	2/12 (16.7)	0 (0)	0 (0)	0 (0)	2 (16.7)
Adenosquamous	1/4 (25.0)	0 (0)	0 (0)	0 (0)	1 (25.0)
Bronchoalveolar	1/8 (12.5)	0 (0)	0 (0)	0 (0)	1 (12.5)
Large cell	0/8 (0.0)	0 (0)	0 (0)	0 (0)	0 (0)
Mucinous adenocarcinoma	1/2 (50.0)	0 (0)	0 (0)	0 (0)	1 (50.0)
Papillary adenocarcinoma	0/4 (0.0)	0 (0)	0 (0)	0 (0)	0 (0)
Normal lung	6/20 (30.0)	0 (0)	2 (10.0)	1 (5.0)	3 (15.0)
Small cell	2/16 (12.5)	0 (0)	0 (0)	1 (6.3)	1 (6.3)
Squamous	35/64 (54.7)	6 (9.5)	4 (6.3)	8 (12.7)	17 (26.6)
Grade					
1	8/19 (42.1)	0 (0)	0 (0)	2 (10.5)	6 (31.6)
2	32/85 (37.6)	6 (7.1)	4 (4.7)	6 (7.1)	16 (18.8)
3	12/23 (52.2)	0 (0)	1 (4.3)	3 (13.0)	8 (34.8)
4	0 (0)	0 (0)	0 (0)	0 (0)	0 (0)
Stage					
I	26/74 (35.1)	4 (5.4)	3 (4.1)	4 (5.4)	15 (20.3)
II	9/38 (23.7)	0 (0)	1 (2.6)	0 (0)	8 (21.1)
III	23/62 (37.1)	2 (3.2)	1 (1.6)	8 (12.9)	12 (19.4)
IV	1/4 (25.0)	0 (0)	0 (0)	0 (0)	1 (25.0)
T					
1	6/24 (25.0)	0 (0)	3 (12.5)	0 (0)	3 (12.5)
2	32/98 (32.7)	6 (6.1)	1 (1.0)	4 (4.1)	21 (21.4)
3	17/48 (35.4)	0 (0)	0 (0)	6 (14.6)	10 (20.8)
4	4/8 (50.0)	0 (0)	1 (12.5)	1 (12.5)	2 (25.0)
N					
0	30/92 (32.6)	4 (4.3)	3 (3.3)	6 (6.5)	17 (18.5)
1	23/68 (33.8)	0 (0)	2 (2.9)	5 (7.4)	16 (23.5)
2	6/20 (30.0)	2 (10.0)	0 (0)	1 (5.0)	3 (15.0)
M					
0	58/176 (33.0)	6 (3.4)	5 (2.8)	12 (6.8)	35 (19.9)
1	1/4 (25.0)	0 (0)	0 (0)	0 (0)	1 (25.0)

Staining intensity was scored on a scale of 0-3 with a score of 3 having the strongest staining for MARCKS. Images were captured at x100 on a Zeiss Observer A1 microscope using an AxioCam MRc 5 camera.

carcinoma, 8 large cell carcinoma, 2 mucinous adenocarcinoma, 20 normal lung, 4 papillary adenocarcinoma, 16 small cell carcinoma, and 64 squamous cell carcinoma tissue samples using Biomax nomenclature (Table I). The TMA was stained for MARCKS and scored in a blinded fashion using a 0-3 scale as indicated in Fig. 1A. MARCKS could be detected in most of the lung cancer histologies represented, but was positive in a minority of the samples overall (Table I). Squamous cell carcinoma had the highest percentage of samples stain for MARCKS and there was a wide range of staining intensities.

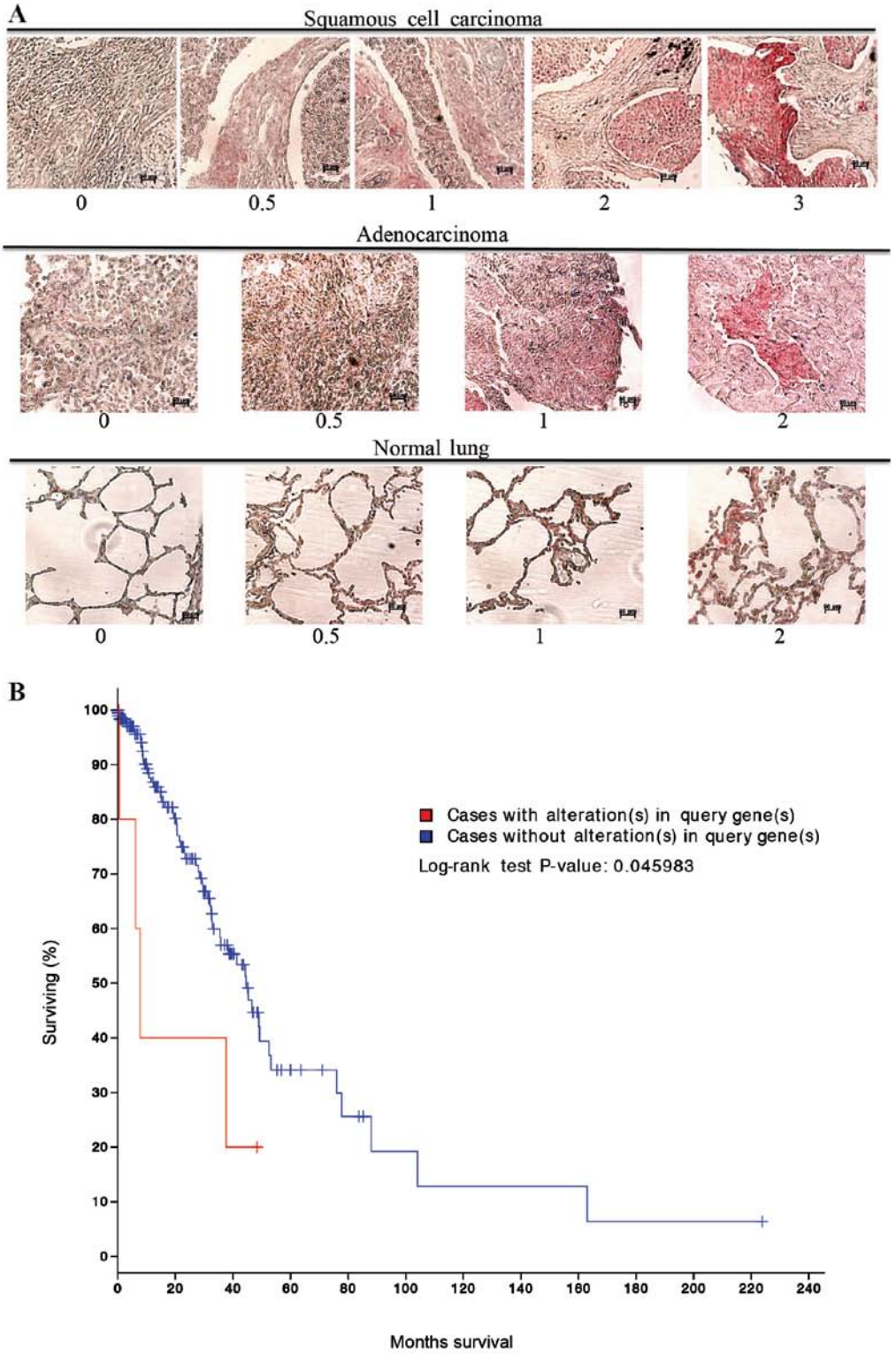

Figure 1. MARCKS protein expression and genetic alterations in human lung cancer. (A) A Biomax Inc. lung tumor tissue microarray was stained for MARCKS and representative tissue images and scoring (indicated below each image) are shown for squamous cell carcinoma (top panel), adenocarcinoma (middle panel), and normal lung tissue (lower panel). (B) Kaplan-Meier survival curve of The Cancer Genome Atlas lung adenocarcinoma dataset comparing survival of patients with MARCKS gene alterations vs. patients without alterations (www.cBioPortal.com). The Kaplan-Meier method was used to obtain estimates of survival, and survival curves were compared using the log-rank test (P-value shown).

For the squamous cell carcinoma samples: 6 tumors had the highest intensity scoring of 3, 4 had an intensity score of 2, 8 scored an intensity of 1, and 17 cases scored a 0.5. In total, 35 out of 64 (54.7%) squamous cell carcinoma cases stained positive for MARCKS expression. In contrast, adenocarcinomas had lower staining percentage and lower staining intensity compared to squamous cell carcinoma. Overall, 17 out of 62 (27.4%) adenocarcinoma samples stained positive for MARCKS though most of them were of 0.5 score (Table I and Fig. 1A). The remaining tumor histologies had a much lower

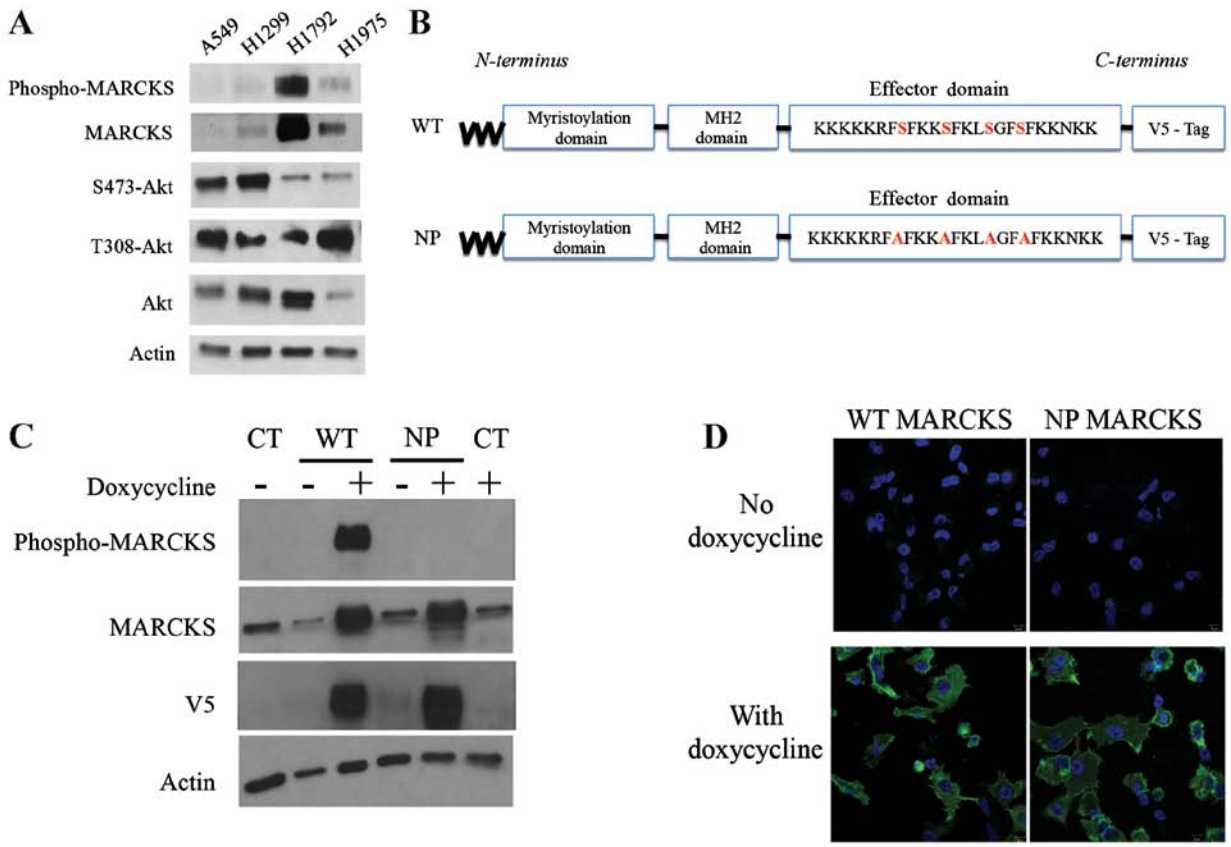

Figure 2. MARCKS and MARCKS mutant overexpression in lung cancer cell lines. (A) A549, H1299, H1792 and H1975 lung cancer cell lines were probed by western blot analysis for phospho-MARCKS, MARCKS, Ser473-Akt, Thr308-Akt, Akt and actin. (B) A schematic diagram depicts the mutant MARCKS constructs. MARCKS contains an N-terminal myristoylation domain, an MH2 domain and an effector domain (ED). The wild-type (WT)-MARCKS and non-phosphorylatable (NP)-MARCKS constructs as designed also contained a C-terminal V5 tag for differentiation from endogenous protein. The NP-MARCKS four serine residues in the ED region were mutated to alanines (indicated in red). (C) Western blot analysis of stably selected A549 cells with control lentiviral (CT), WT or NP MARCKS doxycycline-inducible expression. Cells were cultured with (+) or without (-) doxycycline for 18 h before western blotting. MARCKS, phospho-MARCKS, V5 and actin antibodies were used. (D) V5 tagged wild-type MARCKS (WT MARCKS) or non-phosphorylatable MARCKS (NP MARCKS) stably infected (by lentivirus) A549 cells were treated without (upper panel) or with (lower panel) 2 μg/ml doxycycline to induce expression. Shown are confocal immunofluorescent images of anti-V5 (green) and DAPI nuclear staining (blue) as merged images.

rate of MARCKS staining. Notably, in normal lung tissue 2 samples had a staining intensity of 2, 1 sample had a staining intensity of 1, and 3 samples had a staining intensity of 0.5. In total, 6 out of 20 (30.0%) normal lung samples stained positive for MARCKS (Table I and Fig. 1A). cBioPortal (www.cbioportal.org) (27,28) analysis of The Cancer Genome Atlas (TCGA) dataset for lung adenocarcinomas showed that alterations in the MARCKS gene were associated with a significant (P=0.046) decrease in survival (Fig. 1B).

MARCKS manipulation in lung cancer cells. In order to study the importance of MARCKS in lung cancer, we analyzed several lung cancer cell lines for MARCKS protein expression. Western blotting was performed and revealed that A549 and H1299 human lung cancer cell lines expressed low levels of MARCKS. Alternatively, the human lung cancer cell lines H1792 and H1975 expressed higher levels of MARCKS (Fig. 2A). Therefore, we selected A549 for overexpression of wild-type (WT) and non-phosphorylatable (NP) MARCKS (shown schematically in Fig. 2B). Lentiviral particles were used to establish WT-MARCKS and NP-MARCKS overexpression in A549 cells under the regulation of a tetracycline-inducible promoter as shown by western blotting (Fig. 2C). Because MARCKS phosphorylation has been associated with its cytoplasmic localization (29), the NP-MARCKS construct (shown schematically in Fig. 2B) should remain membrane bound and more effectively sequester PIP_2 than the WT-MARCKS. As such, we used confocal immunofluorescence (Fig. 2D) to determine the subcellular localization of WT-MARCKS vs. NP-MARCKS by probing for the V5 epitope. Indeed confocal imaging shows that WT-MARCKS was expressed predominately in the cytoplasm while the NP-MARCKS construct was predominately localized to the plasma membrane region of the cell.

NP-MARCKS decreases survival after radiation. The iCELLigence real-time impedance assay system (ACEA) was used to screen for cell physiological differences between WT-MARCKS and NP-MARCKS (Fig. 3A), particularly after irradiation as MARCKS knockdown has been shown to promote radiation resistance in GBM (3). Both WT-MARCKS and NP-MARCKS samples were plated and had very similar Cell index (impedance) measurements for the first 6 h. After 6 h, all WT-MARCKS and NP-MARCKS cells were dosed with or without doxycycline overnight. The following morning sham or 5 Gy of irradiation was administered to the

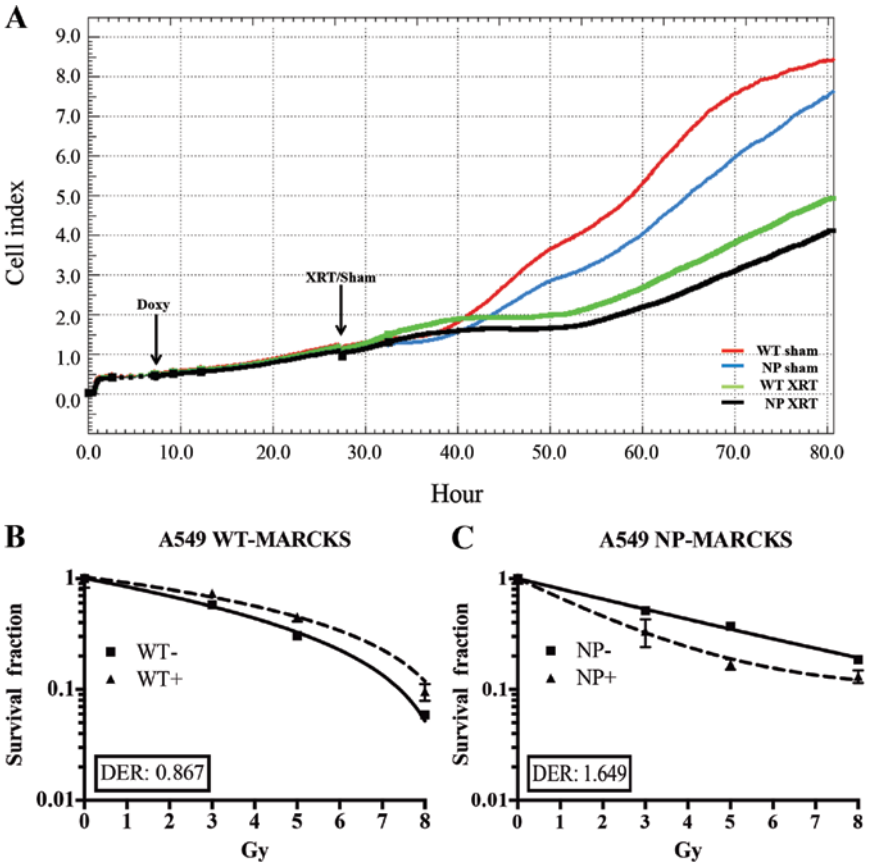

Figure 3. NP-MARCKS overexpression alters the cellular function of A549 cells. (A) The Cell index of doxycycline-induced A549 WT-MARCKS was measured with sham or 5 Gy of irradiation similarly to induced A549 NP-MARCKS under identical conditions. Time of doxycycline induction and radiation are indicated on the graph by the arrows. Cell index mean and standard deviation are shown. (B) A clonogenic assay of A549 WT-MARCKS cells with (+) or without (-) doxycycline-induced overexpression. DER, dose enhancement ratio for a surviving fraction of 0.2. Data are expressed as means ± SEM. (C) A549 NP-MARCKS with (+) and without (-) doxycycline induction were treated and colonies counted using a clonogenic assay (P<0.01). DER, dose enhancement ratio.

cells. After two days of monitoring, we observed that both the WT-MARCKS and NP-MARCKS irradiated groups had lower Cell index measurements compared to their sham counterparts (Fig. 3A). In particular, the NP-MARCKS irradiated cells had the lowest Cell index measurements overall. To confirm these findings, A549 WT-MARCKS were cultured in standard culture media without doxycycline (WT^- or NP^-) or standard culture media with 2 μg/ml of doxycycline (WT^+ or NP^+) for 18 h prior to performance of a clonogenic assay, the gold standard assay for determining radiation sensitivity (30). Two-way ANOVA testing calculated no significant difference between the WT-MARCKS (-) and WT-MARCKS (+) groups (Fig. 3B). We postulated the lack of radiation enhancement could be due to lack of membrane binding (needed for PIP_2 sequestration) of WT-MARCKS. In contrast to WT-MARCKS, we observed a significant decrease in survival with NP-MARCKS overexpression (P=0.01; two-way ANOVA) (Fig. 3C). Overexpression of NP-MARCKS had a radiation sensitizing effect on the A549 cells with a DER of 1.649. This experiment was repeated five times and similar trends were observed.

Impaired DNA damage repair with NP-MARCKS overexpression. Previously, we have observed that overexpression of wild-type MARCKS in GBM cells led to a state of cellular senescence (3). To rule out senescence being the cause of lower clonogenicity seen with NP-MARCKS expression, we measured β-galactosidase, an enzyme upregulated during senescence. Comparing WT-MARCKS with (+) and without (-) doxycycline along with NP-MARCKS with (+) and without (-) doxycycline there was no significant differences in β-galactosidase positive cells 8 days post the 5 Gy irradiation (Fig. 4A). In addition, we examined for mitotic catastrophe following radiation exposure of these cells. Again, comparing WT-MARCKS with (+) and without (-) doxycycline along with NP-MARCKS with (+) and without (-) doxycycline there was no significant mitotic catastrophe difference over the course of 96 h post the 5 Gy irradiation (Fig. 4B). As we observed no difference in senescence or mitotic catastrophe, we anticipated that NP-MARCKS was influencing DNA damage compared to WT-MARCKS. As shown in Fig. 4C, DNA damage was studied by probing for DNA double-strand breaks (DSB) by measuring γH2AX foci (26). As expected, irradiation of A549 cells increased γH2AX foci formation within 1-h post irradiation. At 24 h, all groups approached basal level γH2AX foci formation except for NP-MARCKS (+) overexpressing cells that demonstrated persistent γH2AX foci staining, suggesting that NP-MARCKS promotes prolonged DNA damage, leading to a decrease in cell survival following radiation exposure.

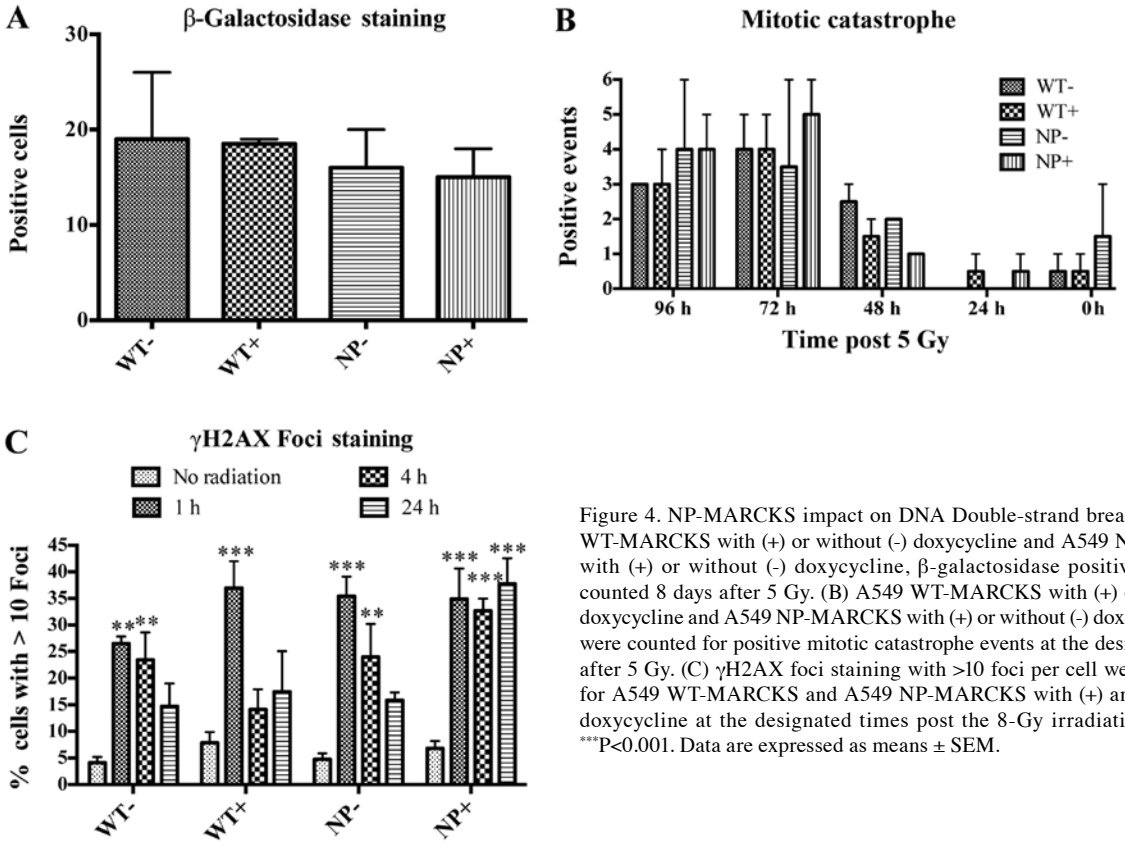

Figure 4. NP-MARCKS impact on DNA Double-strand breaks. (A) A549 WT-MARCKS with (+) or without (-) doxycycline and A549 NP-MARCKS with (+) or without (-) doxycycline, β-galactosidase positive cells were counted 8 days after 5 Gy. (B) A549 WT-MARCKS with (+) or without (-) doxycycline and A549 NP-MARCKS with (+) or without (-) doxycycline cells were counted for positive mitotic catastrophe events at the designated times after 5 Gy. (C) γH2AX foci staining with >10 foci per cell were calculated for A549 WT-MARCKS and A549 NP-MARCKS with (+) and without (-) doxycycline at the designated times post the 8-Gy irradiation. **P<0.01; ***P<0.001. Data are expressed as means ± SEM.

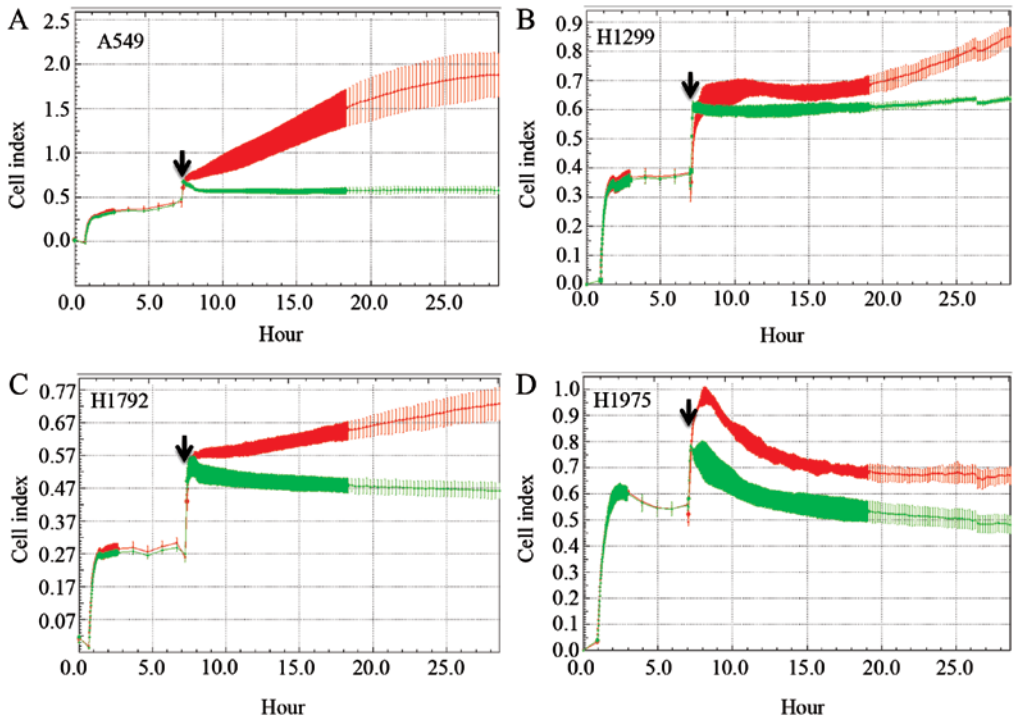

Figure 5. A MARCKS ED peptide mimetic impairs the lung cancer Cell index. Lung cancer cell lines (A) A549; (B) H1299; (C) H1792; (D) H1975 were plated 6 h before the addition of 25 μM of control peptide (red) or MARCKS ED peptide (green). Arrow indicates the time at which peptides were added to the culture. Cell index mean and standard deviation are shown.

Using a MARCKS ED-targeting peptide mimetic in lung cancer cells. Because MARCKS has no enzymatic activity, we utilized a peptide mimetic to modulate MARCKS behavior by targeting the ED of MARCKS. We engineered a cell permeable peptide mimetic composed of the cell permeable TAT peptide conjugated to the 25 amino acid sequence (KKKKKR

FSFKKSFKLSGFSFKKNKK) of the ED region of MARCKS (19). A control peptide was generated based on the Expasy random peptide generator using the average amino acid composition computed from Swiss-Prot (CEIEEHAWNTV EMFSSFPGTQLYNDA). This sequence was also conjugated to TAT. A549, H1299, H1792 and H1975 lung cancer cell lines were plated in the iCELLigence instrument for a proliferation experiment with the MARCKS-ED or control peptide. In all four cell lines, the control peptide group had an increased Cell index over the duration of the assay (Fig. 5). However, the MARCKS-ED TAT peptide treated cells showed a marked decrease in their Cell index, suggesting that targeting the MARCKS ED is a potential strategy against lung cancer.

Discussion

The role of MARCKS in the development and progression of cancer is quite controversial in that there is evidence for both tumor suppression (1-5) and tumor promotion (6,7). As we have previously postulated (3), the cellular environment and co-existent signaling pathways almost certainly contribute to the importance and role of MARCKS. In the present study, we identified a key role of the ED of MARCKS in terms of cellular response, particularly to radiation. The ED of MARCKS is a very important domain as it determines MARCKS subcellular localization, binds PIP_2 and F-actin allowing MARCKS to influence both proliferation and migration of cancer cells. Intrinsic modulators of the ED of MARCKS include serine kinases, including PKCs and ROCKs, as well as calcium-calmodulin (Ca^{2+}-CAM), which bind in a mutually exclusive manner. Indeed, when we induced expression of a non-phosphorylatable MARCKS (that should not bind Ca^{2+}-CAM either), we noted radiation sensitization concomitant with a prolongation of DNA double strand breaks. Treatment with a peptide mimetic of the ED was effective in blocking tumor cell growth as well. These findings complement our previous work in GBM cell lines (3) showing that loss of MARCKS promotes radiation protection and increased cell growth, while overexpression of MARCKS suppressed growth.

Recent studies of MARCKS in lung cancer have also suggested that interfering with the N-terminal region of MARCKS can manipulate cellular behavior. An N-terminal peptide mimetic corresponding to the first 24 amino acids of MARCKS reduced levels of phospho-MARCKS and inhibited cellular migration (18). A proposed mechanism for a peptide mimetic interfering with MARCKS function is that the peptide therapy overwhelms the cell and prevents MARCKS from cycling to and from the plasma membrane. This proposed mechanism is consistent with the decreased levels of phospho-MARCKS observed in our studies. Several studies have shown that phosphorylated MARCKS (cytoplasmic localization) promotes cancer cell migration (7,31). The role of MARCKS expression and subcellular localization upon cell migration is reported to be influenced by the cycling of MARCKS from the plasma membrane to the cytoplasm and back to the plasma membrane (32), which is consistent with our observations. Additionally, MARCKS contains two actin binding sites in the ED, that are disrupted by ED phosphorylation, thus preventing cross-linking (33). MARCKS may have additional indirect effects on this process since actin-binding proteins, such as Arp2/3 and N-WASP, bind to PIP_2, once again, pointing to the importance of the ability of MARCKS to sequester the phospholipid (34).

Additionally, we describe here the expression pattern of the MARCKS protein in a variety of human lung tumor histologies. To the best of our knowledge, the present study is the first to report such findings. MARCKS expression was predominately expressed in the adenocarcinoma and squamous cell carcinoma tumor samples. Other cases, including small cell carcinoma and atypical carcinoid had very few samples that stained positive for MARCKS. Currently, we cannot comment on clinical outcomes relative to MARCKS protein expression since the TMA lacked outcome data. However, as discussed above, the cellular response to MARCKS expression will depend on its phosphorylation status and cellular localization, which has not been consistently examined in clinical specimens. For example Hanada *et al* (17) described that squamous cell carcinomas with higher MARCKS expression had poorer prognosis, yet, neither phosphorylation status or subcellular location was described. Future work on MARCKS, particularly in lung cancer, will require a more in depth investigation beyond gene expression or protein expression levels to include the status of MARCKS modulators and ED phosphorylation.

Acknowledgements

We would like to thank Shawn Williams for his assistance with the confocal microscopy. Funding sources included: UAB Radiation Oncology Intramural Pilot Grant (awarded to T.D.R. and C.D.W.); UAB Brain SPORE Pilot Project (awarded to C.D.W.); and ASTRO Junior Faculty Training Research Award (awarded to C.D.W.).

References

1. Bickeboller M, Tagscherer KE, Kloor M, *et al*: Functional characterization of the tumor-suppressor MARCKS in colorectal cancer and its association with survival. Oncogene: 24 March, 2014 (Epub ahead of print). doi: 10.1038/onc.2014.40.
2. Brooks G, Brooks SF and Goss MW: MARCKS functions as a novel growth suppressor in cells of melanocyte origin. Carcinogenesis 17: 683-689, 1996.
3. Jarboe JS, Anderson JC, Duarte CW, *et al*: MARCKS regulates growth and radiation sensitivity and is a novel prognostic factor for glioma. Clin Cancer Res 18: 3030-3041, 2012.
4. Li T, Li D, Sha J, Sun P and Huang Y: MicroRNA-21 directly targets MARCKS and promotes apoptosis resistance and invasion in prostate cancer cells. Biochem Biophys Res Commun 383: 280-285, 2009.
5. Masaki T, Tokuda M, Yoshida S, *et al*: Comparison study of the expressions of myristoylated alanine-rich C kinase substrate in hepatocellular carcinoma, liver cirrhosis, chronic hepatitis, and normal liver. Int J Oncol 26: 661-671, 2005.
6. Browne BC, Hochgräfe F, Wu J, *et al*: Global characterization of signalling networks associated with tamoxifen resistance in breast cancer. FEBS J 280: 5237-5257, 2013.
7. Techasen A, Loilome W, Namwat N, *et al*: Myristoylated alanine-rich C kinase substrate phosphorylation promotes cholangiocarcinoma cell migration and metastasis via the protein kinase C-dependent pathway. Cancer Sci 101: 658-665, 2010.
8. Janku F, Garrido-Laguna I, Petruzelka LB, Stewart DJ and Kurzrock R: Novel therapeutic targets in non-small cell lung cancer. J Thorac Oncol 6: 1601-1612, 2011.
9. Newton AC: Lipid activation of protein kinases. J Lipid Res 50 (Suppl) S266-S271, 2009.

10. Engelman JA: Targeting PI3K signalling in cancer: opportunities, challenges and limitations. Nat Rev Cancer 9: 550-562, 2009.
11. Ellena JF, Burnitz MC and Cafiso DS: Location of the myristoylated alanine-rich C-kinase substrate (MARCKS) effector domain in negatively charged phospholipid bicelles. Biophys J 85: 2442-2448, 2003.
12. Wang J, Gambhir A, Hangyas-Mihalyne G, Murray D, Golebiewska U and McLaughlin S: Lateral sequestration of phosphatidylinositol 4,5-bisphosphate by the basic effector domain of myristoylated alanine-rich C kinase substrate is due to nonspecific electrostatic interactions. J Biol Chem 277: 34401-34412, 2002.
13. Tanabe A, Kamisuki Y, Hidaka H, Suzuki M, Negishi M and Takuwa Y: PKC phosphorylates MARCKS Ser159 not only directly but also through RhoA/ROCK. Biochem Biophys Res Commun 345: 156-161, 2006.
14. Thelen M, Rosen A, Nairn AC and Aderem A: Regulation by phosphorylation of reversible association of a myristoylated protein kinase C substrate with the plasma membrane. Nature 351: 320-322, 1991.
15. Clarke PR, Siddhanti SR, Cohen P and Blackshear PJ: Okadaic acid-sensitive protein phosphatases dephosphorylate MARCKS, a major protein kinase C substrate. FEBS Lett 336: 37-42, 1993.
16. Stumpo DJ, Graff JM, Albert KA, Greengard P and Blackshear PJ: Molecular cloning, characterization, and expression of a cDNA encoding the '80- to 87-kDa' myristoylated alanine-rich C kinase substrate: a major cellular substrate for protein kinase C. Proc Natl Acad Sci USA 86: 4012-4016, 1989.
17. Hanada S, Kakehashi A, Nishiyama N, *et al*: Myristoylated alanine-rich C-kinase substrate as a prognostic biomarker in human primary lung squamous cell carcinoma. Cancer Biomark 13: 289-298, 2013.
18. Chen CH, Thai P, Yoneda K, Adler KB, Yang PC and Wu R: A peptide that inhibits function of Myristoylated Alanine-Rich C Kinase Substrate (MARCKS) reduces lung cancer metastasis. Oncogene 33: 3696-3706, 2013.
19. Graff JM, Rajan RR, Randall RR, Nairn AC and Blackshear PJ: Protein kinase C substrate and inhibitor characteristics of peptides derived from the myristoylated alanine-rich C kinase substrate (MARCKS) protein phosphorylation site domain. J Biol Chem 266: 14390-14398, 1991.
20. Solly K, Wang X, Xu X, Strulovici B and Zheng W: Application of real-time cell electronic sensing (RT-CES) technology to cell-based assays. Assay Drug Dev Technol 2: 363-372, 2004.
21. Nam HY, Han MW, Chang HW, *et al*: Radioresistant cancer cells can be conditioned to enter senescence by mTOR inhibition. Cancer Res 73: 4267-4277, 2013.
22. Jarboe JS, Jaboin JJ, Anderson JC, *et al*: Kinomic profiling approach identifies Trk as a novel radiation modulator. Radiother Oncol 103: 380-387, 2012.
23. Tu T, Thotala D, Geng L, Hallahan DE and Willey CD: Bone marrow X kinase-mediated signal transduction in irradiated vascular endothelium. Cancer Res 68: 2861-2869, 2008.
24. Yang ES, Wang H, Jiang G, *et al*: Lithium-mediated protection of hippocampal cells involves enhancement of DNA-PK-dependent repair in mice. J Clin Invest 119: 1124-1135, 2009.
25. Nowsheen S, Bonner JA and Yang ES: The poly(ADP-Ribose) polymerase inhibitor ABT-888 reduces radiation-induced nuclear EGFR and augments head and neck tumor response to radiotherapy. Radiother Oncol 99: 331-338, 2011.
26. Yang ES, Nowsheen S, Wang T, Thotala DK and Xia F: Glycogen synthase kinase 3beta inhibition enhances repair of DNA double-strand breaks in irradiated hippocampal neurons. Neuro Oncol 13: 459-470, 2011.
27. Gao J, Aksoy BA, Dogrusoz U, *et al*: Integrative analysis of complex cancer genomics and clinical profiles using the cBioPortal. Sci Signal 6: pl1, 2013.
28. Cerami E, Gao J, Dogrusoz U, *et al*: The cBio cancer genomics portal: an open platform for exploring multidimensional cancer genomics data. Cancer Discov 2: 401-404, 2012.
29. Ohmori S, Sakai N, Shirai Y, *et al*: Importance of protein kinase C targeting for the phosphorylation of its substrate, myristoylated alanine-rich C-kinase substrate. J Biol Chem 275: 26449-26457, 2000.
30. Franken NA, Rodermond HM, Stap J, Haveman J and van Bree C: Clonogenic assay of cells in vitro. Nat Protoc 1: 2315-2319, 2006.
31. Chen X and Rotenberg SA: PhosphoMARCKS drives motility of mouse melanoma cells. Cell Signal 22: 1097-1103, 2010.
32. Disatnik MH, Boutet SC, Pacio W, *et al*: The bi-directional translocation of MARCKS between membrane and cytosol regulates integrin-mediated muscle cell spreading. J Cell Sci 117: 4469-4479, 2004.
33. Yarmola EG, Edison AS, Lenox RH and Bubb MR: Actin filament cross-linking by MARCKS: characterization of two actin-binding sites within the phosphorylation site domain. J Biol Chem 276: 22351-22358, 2001.
34. Kalwa H and Michel T: The MARCKS protein plays a critical role in phosphatidylinositol 4,5-bisphosphate metabolism and directed cell movement in vascular endothelial cells. J Biol Chem 286: 2320-2330, 2011.